ISSN 1392–1207. MECHANIKA. 2018 Volume 24(1): 149–154

Effect of Temperatures and Pulling Rates on Microstructure and Mechanical Properties of 6061 Aluminium Alloy in Directional Solidification

Tao HE, Li MIN, Yuan ming HUO, Hong Jun LIU, Xiao jie YI
College of Mechanical Engineering, Shanghai University of Engineering Science, Shanghai 201620, China,
E-mail: hetao@sues.edu.cn

crossref http://dx.doi.org/10.5755/j01.mech.24.1.19499

1. Introduction

As Al-Mg-Si series alloy, 6061 aluminium alloy has good mechanical processing performance and is widely used in aerospace construction and other industries [1]. The mechanical properties of material are determined by its microstructure. And, processing parameters of directional solidification can be controlled to change microstructure and then enhance the performance of 6061 aluminium alloy [2].

As early as the 1950s, Versnyder et al. [3] developed a top-down temperature gradient using the heat-generating method. Since it is not possible to ensure the repeated production of high quality castings, Versnyder et al. [4-5] proposed a directional solidification power reduction in the 1960s. However, its' thermal conductivity is still unsatisfactory. High-speed solidification method is proposed by Erickson et al. [5] in 1971. Unfortunately, the temperature gradient is not large enough. Giamei et al. [6] invented a liquid metal cooling (LMC) method in 1976, which is not only relatively inexpensive but also suitable for industrial production.

Many articles were published to study microstructure change in directional solidification. Wang et al. [7] prepared Al-13.6Cu-6Si ternary eutectic organization. It was found that the pulling rates in directional solidification greatly improved the hardness and tensile resistance of the alloy. Li et al. [8] studied the microstructure change of Al-Cu alloy under different temperature gradient using directional solidification device, and found that there was a transition between dendritic growth and cellular growth. Wu et al. [9] prepared Al-4.5wt % Cu alloy at different pulling rates (from 20 μm/s to 220 μm/s). It was found that the dendrite spacing decreases with the increase of the pulling rates, which is more obvious when pulling rate was less than 100μm/s. Liu et al. [10-13] also investigated the effect of different pulling rates on Al-5wt % Cu in directional solidification. It was found that the solidification rate increases with the increase of the pulling rates. Furthermore, the solidified structure changed from cellular crystals to dendrites crystals, and the dendrites gradually were refined. As for directional solidification of 6061 aluminium alloy, few researchers have studied the effect of temperatures and pulling rates on microstructure and mechanical properties.

The aim of this article is to study the effect of temperatures and pulling rates on microstructure and mechanical properties of 6061 aluminium alloy using Bridgman-type vacuum furnace with LMC method. Firstly, directional solidification experiment was conducted at different temperatures and pulling rates to prepare 6061 aluminium alloy rods. Secondly, microstructure of 6061 aluminium alloy rods was investigated using SEM. Thirdly, tensile tests and microhardness tests were carried out for 6061 aluminum alloy rods. Finally, experimental results were discussed by comparing experimental data.

The directional solidification experiment was carried out in a Bridgman-type vacuum furnace with LMC method, as shown in Fig. 1. The 6061 aluminum rods were selected as original material in the directional solidification experiment. The chemical composition of 6061 aluminum alloy is shown in Table. The crucible was made of Al2O3corundum tube with purity. The heating method was resistance heating. The main procedure of LMC directional solidification includes two steps: (1) put the 6061 aluminum alloy rod into the heat preservation furnace within the corundum tube mold and thermal insulation for a period of time; (2) according to the given pulling rate, 6061 aluminum alloy rods finally were immersed into Ga-Sn liquid for cooling.

The furnace was firstly evacuated and then filled with high purity argon gas. The specimens were initially heated up to 300 °C at a pre-set heating rate in an alundum tube, and then held isothermally for 35 min at 300 °C in the thermal insulation baffle. The detailed process of directional solidification was carried out with three steps: Firstly, in order to obtain a stable temperature field, the bottom of the specimens was pulled downwards into Ga-In liquid metal about 10 mm with a pre-set pulling rate, and then hold for 5 min. Secondly, a stable directional solidified zone of 30 mm was obtained at pre-set pulling rates. Thirdly, water quenching was performed to reserve the morphology of the solid/liquid interface with different pulling rates by operating drawing bar.

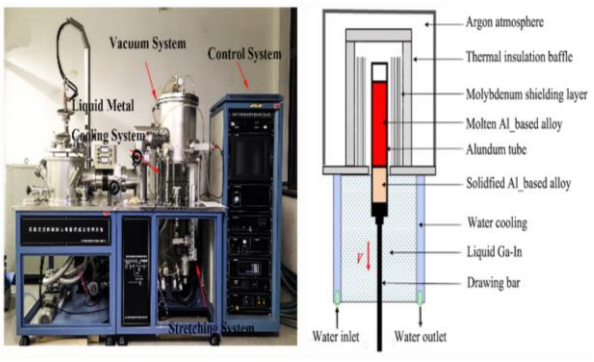

a b

Fig. 1 (a) Experimental equipment of directional solidification, (b) Schematic illustration of the Bridgman - type direction also solidification apparatus

Table

The chemical compositions of 6061 aluminum alloy (mass fraction %)

Al	Si	Fe	Cu	Mn	Mg	Cr	Zn	Ti
>97.01	0.58	0.41	0.3	<0.15	1	0.3	<0.2	<0.05

During directional solidification, temperatures were changed from 700°C to 800°C and the pulling rates from 20 μm/s to 150 μm/s, so that different 6061 aluminium alloy specimens can be obtained to study the effect of temperatures and pulling rates on microstructure and mechanical properties. Experimental specimens were prepared as shown in Fig. 2.

Fig. 2 Experimental specimens

2. Testing procedures

Testing procedure of $J-R$ curve is described in the American standard ASTM E1152-87 [1]. In the majority of tests compact specimens *C*(*T*) for tension or *B*(*T*) for bending are applied. Compact specimens (Fig. 1) of different sizes are applied. The standard offers the following thickness of specimens: 1/2*T*, 1*T*, 2*T* and 4*T*, where *T*=25.4 mm. The specimens have three basic sizes: length of a crack a, thickness *B* and width *W*. In many cases there are accepted *W*=2*B* and *a*/*W*>0.5. Basic sizes of specimens' *B* and *W*-*a* should exceed the size of plastic zone in advance of a developing crack minimum 50 times, otherwise the incorrect characteristics of fracture toughness will be received. Sizes of the test specimens depend on the thickness of material; from which they are made. Specimens of the size 1/2*T* and 1*T* have been used in our test, because the diameter of steam pipes.

Factor of load asymmetry in cycle during precracking should not exceed $r \le 0.1$ and the length of a crack should not be less than 5% from a_0, but not less than 1.3 mm. Beside the definition of $J-R$ by the method of a compliance requires to observe condition $0.5 < a_0/W < 0.75$, where a_0 is the distance from loading line up to the top of a crack. At $a_0/W < 0.5$ the method of compliance loses sensitivity, and at $a_0/W > 0.75$ the plastic zone will be much more increased and becomes too large. So, the ratio a_0/W in our experiments varied within the limits 0.5-0.75.

In order to facilitate the observation, specimens were sectioned and polished as small squares of 8 mm from 6061 aluminium alloy casting rods. The observed specimens were cleaned with alcohol by ultrasonic cleaners. And, then the observed specimens were put into the mixture solution (1.0 ml HF, 1.5 ml HCL, 2.5 ml HNO3, 65 ml H2O) for 10 seconds to reveal the microstructure. The microstructure of specimens was observed using Hitachi SU8070 SEM.

Tensile specimens were prepared by cutting from 6061 aluminium alloy casting rods after directional solidification along the longitudinal direction using a spark cutter. The shape and dimension of tensile specimens are shown in Fig. 3. Tensile specimens were polished on the abrasive paper to remove the cutting marks completely to prevent stress concentration and cracks formation during the tensile tests.

Tensile tests were conducted on a JVJ-50s microcomputer controlled electronic universal testing machine at a pulling speed of 3 mm/min under the room temperature. Stress curves were measured during tensile tests. Tensile specimens were stretched to failure for three times with the same process parameters, and the average value of experimental data was taken as the final result.

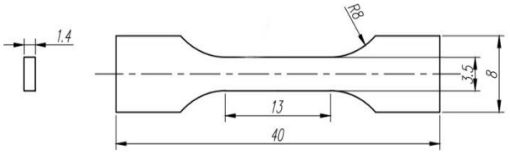

Fig. 3 The shape and dimensions of tensile specimens

Wire Cut Electric Discharge Machine was used to prepare the cylinder specimens with the length of 12 mm and the diameter of 10 mm. The polished specimens were put into alcohol, cleaned with an ultrasonic cleaner, and dried by a blower. Then specimens were placed on MHVD-1000IS digital microhardness tester. Seven random points within specimens were selected to measure the microhardness. Their average value was recorded as the final experimental data.

3. Results and discussion

Fig. 4 shows the effect of temperatures on microstructure of 6061 aluminum alloy after solidification. When the temperature is 700 °C, the dendritic grains grow crossed with each other, shown in Fig. 4, a. It is obvious that they grow in the opposite direction to the heat flow. In Fig. 4, b, the eutectic solidification characteristics of the white α-Al substrate are very obvious at temperature of 750°C and pulling rate of 50 μm/s. The dendritic spacing of Fig. 4, b is smaller than that of Fig. 4, a. That means that the dendritic spacing decreases with the increase of the temperatures, and the dendritic grains become small.

When the temperature is 800°C, microstructure becomes coarse in Fig. 4, c. The lamellar structure of dendritic grains was determined by the solidification process. Dendritic grains grow directionally during solidification, which provides the solidification path [14-18]. The orientation of the lamellar structure is consistent with the direction of grain growth at the pulling rate of 50 μm/s. Meanwhile, dendrite crystal transform to cellular crystal. It can be seen from Fig. 4, c that white α-Al substrate exists significantly. It is because that when the molten metal enters the crystallizer, the chilling layer formed due to the hybrid cooling of Ga-Sn liquid and the water. With the release of latent heat, the solid-liquid interface is easy to decrease under the temperature gradient in a short time. The lateral heat radiation plays a vital role in the orientation of grain growth, which leads to the formation of eutectic compounds [19-25].

The dendritic spacing is large at 700°C. When the temperature is 750°C, the dendritic spacing becomes small. When the temperature reaches 800°C, the dendrite spacing

further reduce. However, a lot of slag inclusions and transgranular cracks are produced at the same time, which may lead to the decline of mechanical properties.

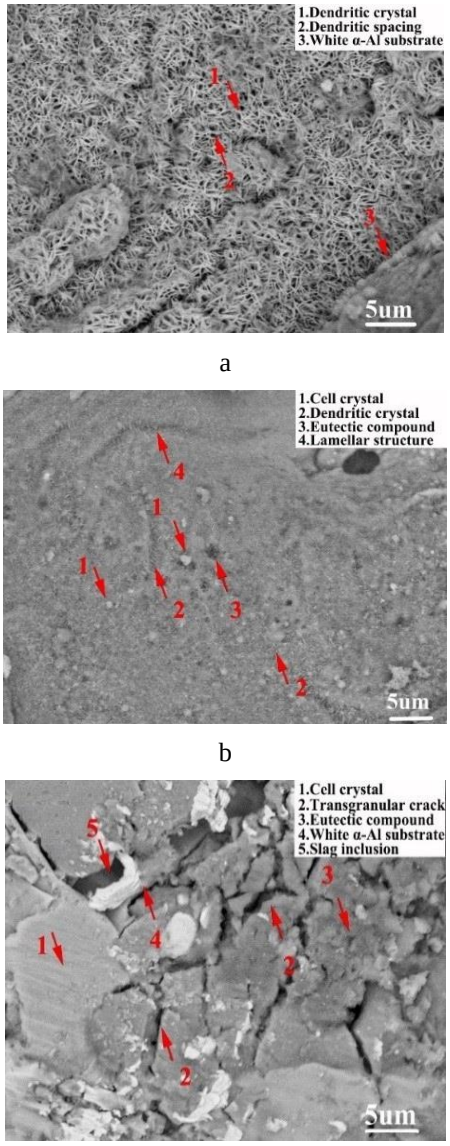

Fig. 4 Microstructure of 6061 aluminum alloy after solidification at the temperatures of: a - 700°C, b - 750°C and c - 800°C) with a pulling rate of 50 μm/s

Liu et al. [26-30] have investigated the influence of temperature gradient on mechanical properties in directional solidification. All the experimental results show that the solidification interface morphology will appear cellular crystal when the temperature reaches a certain value. Meanwhile, the grain structure will become fine, and the mechanical properties are relatively enhanced.

Fig. 5 shows the effect of temperatures on tensile properties of 6061 aluminium alloy after solidification. It can be seen from Fig. 5 that tensile strength and the total elongation are both lower at the temperature of 700°C, whose tensile strength is 82.2 MPa and elongation is 16.7 %. However, the tensile strength at the temperature of 750°C is the highest, reaching 182.51 MPa. Besides, its' elongation reaches 33.68 %. The structure is coarse at the temperature of 800°C, shown in Fig. 4, c. The tensile strength reaches 171.45 MPa, and its' elongation reaches 33.32%. In the process of directional solidification, the temperature gradient is perpendicular to the solid-liquid interface, which provides a formidable power with a single and cycled heat flow. So, some small cracks formed in the 6061 aluminium alloy specimens after solidification at 800°C. Although the grain structure is more refined, those defects have impact on the tensile strength and the total elongation. That is why tensile properties are similar at 750°C and 800°C, shown in Fig. 5.

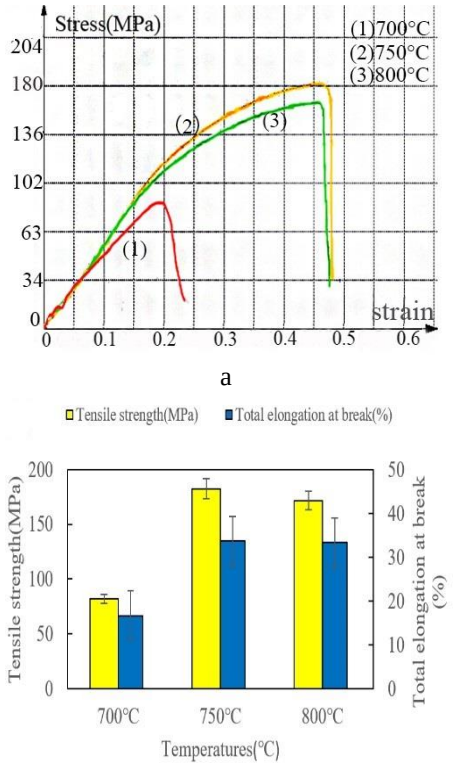

Fig. 5 Effect of temperatures on tensile properties of 6061 aluminum alloy after solidification: a - tensile stress curves, b - tensile peak stress and elongation

Fig. 6 shows the effect of temperatures on microhardness of 6061 aluminium alloy after solidification. It can be seen from Fig. 6 that microhardness of the alloy specimen increases with the increase of temperatures. At the temperature of 700°C, the microhardness reaches 53.18 HV. At the temperature of 750 °C, the microhardness reaches 54.76 HV. The microhardness at the temperature of 800 °C is the highest, reaching 56.77 HV. The reason is that the elevated temperatures lead to subcooling in the solidification, and the increase of the grains nucleation number.

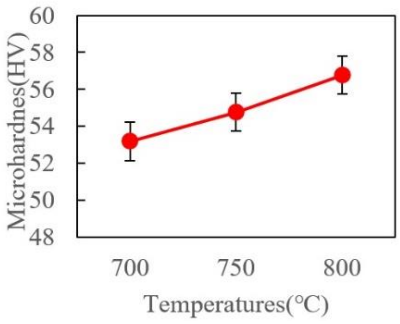

Fig. 6 Effect of temperatures on microhardness of 6061 aluminium alloy after solidification

Wu et al. [31-34] studied the microstructures and mechanical properties of Al-Si-Mg ternary eutectic alloys by changing the pulling rate at a given temperature. It can be found that the solidification structure shows a tendency to refine with the increases of pulling rate. Moreover, the dendrites become smaller and the lamellar spacing is also markedly reduced. Thus, the tensile strength and hardness are reinforced.

Fig. 7 shows the effect of pulling rates on tensile properties of 6061 aluminium alloy after solidification. It is clear that the tensile strength is the highest at the pulling rate of 50 μm/s, reaching 183.31 MPa. Besides, its' elongation reaches the highest value of 37.66%. At the pulling rate of 20 μm/s, the tensile strength reaches 152.86 MPa, and the elongation is 37.14%. At the pulling rate of 100 μm/s, the tensile strength reaches 170.53 MPa, and the elongation is 35.69%. At the pulling rate of 150 μm/s, the tensile strength reaches 182.97 MPa, and the elongation is 37.04%. The difference of elongation is small for different pulling rates.

During directional solidification, both the liquid metal cooling and circulating water cooling greatly accelerate the solidification of the alloy. Therefore, grains within microstructure after solidification are smaller, and the orientation of grain growth is parallel to the direction of the heat flow. The transverse grain boundary disappears. The micocracks without expansion greatly enhance the tensile properties of 6061 aluminum alloy.

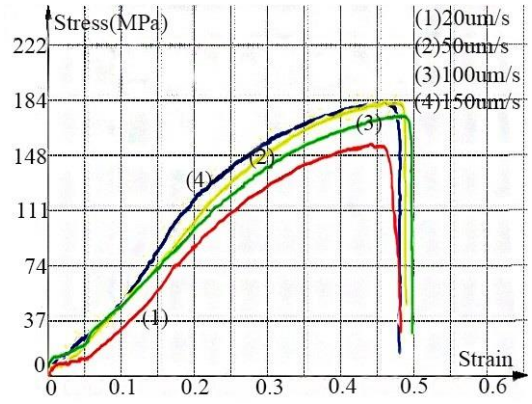

a

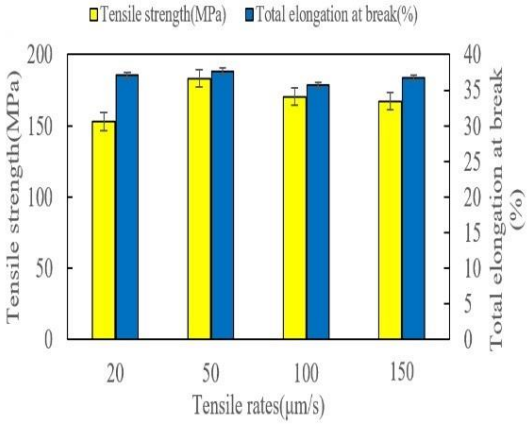

b

Fig. 7 Effect of pulling rates on tensile properties of 6061 aluminum alloy after solidification: a - tensile stress curves, b - tensile peak stress and elongation

Fig. 8 shows the effect of pulling rates on microhardness of 6061 aluminium alloy after solidification. It can be seen from Fig. 8 that microhardness increases with the increase of pulling rates. The highest microhardness reaches 67.66 HV at the pulling rate of 150 μm/s, shown in Fig. 8. At the pulling rate of 20 μm/s and 50 μm/s, the microhardness reaches 56.78 HV and 56.77 HV, respectively. And, the microhardness reaches 61.88HV at the pulling rate of 100 μm/s. The increase of the microhardness is due to the refinement of the microstructure. The Mg2Si compound as strengthening phase was found in the casting 6061 aluminium alloy, whose distribution is more uniform with the increase of the pulling rates. That is why the microhardness of casting 6061 aluminium alloy increases with the increase of pulling rates.

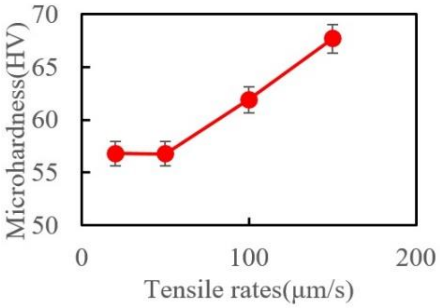

Fig. 8 Effect of pulling rates on microhardness of casting 6061 aluminum alloy after solidification

4. Conclusions

1. With the increase of the temperatures, the dendritic structure of the specimen gradually decreases, and the cellular spacing becomes smaller. Some small defects appear during directional solidification, which results in the decline of mechanical properties of casting 6061 aluminium alloy with the increase of temperatures.

2. The tensile strength at the temperature of 750°C is the highest, reaching 182.51 MPa. Besides, its' elongation reaches 33.68%, and the microhardness reaches 54.76 HV. The microhardness at the temperature of 800°C is the highest, reaching 56.77 HV. The microhardness of casting 6061 aluminum alloy increases with the increases of temperatures.

3. When the pulling rate is 50 μm/s, the tensile strength reaches 183.31 MPa, and elongation reaches 37.66%. Its' tensile strength and elongation are superior to that at the pulling rate of 100 μm/s and 150 μm/s. The microhardness of the casting 6061 aluminium alloy increases with the increase of pulling rates. The highest record of microhardness reaches 67.66 HV at the pulling rate of 150 μm/s.

5. Acknowledgements

This project is funded by Research on Key Technologies of Underwater Vehicles for Deep-sea Oil and Gas Fields (Grant No. 16030501200) and 17KY0106 Prediction of Mechanical Properties of Aluminum Alloy Oriented to Solidification Based on Artificial Neural Network (Grant No. E3-0903-17-01006). The Robot Functional Materials Preparation Laboratory in Shanghai University of Engineering Science is also gratefully acknowledged.

References

1. **Chen, J-H.; Li, M-E.; Yu, J-R.** et al. 2010. Effects of Heat Treatment on Microstructure and Mechanical Properties of 6061 aluminium Alloy, Journal of Lanzhou University of Technology, 36 (2): 15-17. http://www.cqvip.com/read/read.aspx?id=33657622.
2. **Xie, S-K.; Yi, R-X.; Huang, Q.** et al. 2011. Effects of Rare Earth Ce on Fluidity and Hot Tearing Trend of Al4. 5Cu Alloy, Nonferrous Metals (Extractive Metallurgy), 33 (4): 1007-7545. http://www.cqvip.com/read/read.aspx?id=38208243.
3. **Dobrzański, L.; Maniara, R.; Krupiński, M.** et al. 2007. Microstructure and mechanical properties of AC AlSi9CuX alloys, Journal of Achievements in Materials and Manufacturing Engineering, 24 (2): 51-54. http://www.oalib.com/paper/2923835#.Wk8ew-PmWZPY.
4. **Mrówka-Nowotnik, G.; Sieniawski, J.; Wierzbińska, M.** 2007. Analysis of intermetallic particles in AlSi1MgMn aluminium alloy, 20 (1-2): 155-158. http://www.oalib.com/paper/2901531#.Wk8fAP-mWZPY.
5. **Wierzbińska, M, Sieniawski, J.** 2006. Effect of morphology of eutectic silicon crystals on mechanical properties and cleavage fracture toughness of AlSi5Cu1 alloy, Journal of Achievements in Materials and Manufacturing Engineering, 14 (1-2): 31-36. http://www.oalib.com/paper/2901413#.Wk8fLPmWZPY.
6. **Adeosun, S.; Balogun, S.; Osoba, L.** et al. 2011. Effect of Cu and Zn addition on the mechanical properties of structural aluminium alloy, Journal of modern manufacturing technology, 3(1): 103-110. https://www.unilag.edu.ng/opendocnew.php?docname=17822&doctype=pdf.
7. **Wang, Xin; Xu, Rui; Zhang, Jing; Zhao, Xin,** et al. 2011. Directional solidification structure of Al-Cu-Si ternary eutectic alloy, Casting project, 37 (4) :1-5. http://www.cqvip.com/read/read.aspx?id=46795098.
8. **Li, Jianguo; Mao, Xiemin; Fu, Hengzhi.** 1991, Morphological transition in Al-Cu alloy during high gradient orientation solidification, Advances in Materials Science, 5 (6): 461-465. http://www.cnki.com.cn/Article/CJFDTotal-CYJB199106000.htm.
9. **Wu, Qiang; Si, Naichao; Guo, Yi.** 2007. Relationship between Dendritic Microstructures and Drawing Rate of Directionally Solidified Al-4.5% Cu Alloys, Journal of Nonferrous Metals, 17 (7): 1101-1106. https://college.zjut.cc/10299/t/572611.html.
10. **Liu, Haixia; Wu, Qiang; Si, Naichao.** 2005. Effect of different stretching speed of Al-5% Cu on directional solidification, Casting, 54 (1): 40-43. http://www.cnki.com.cn/Article/CJFDTotalZZZZ200501009.html.
11. **Huang, H-F.** 2004. The Influence of Pure Rare Earths Ce on the Castability of Al-4.5％Cu, Mechanical Engineer, (6): 35-36. http://www.cqvip.com/read/read.aspx?id=9907469.
12. **Salishchev, G; Tikhonovsky, M; Shaysultanov, D.** et al. 2014. Effect of Mn and V on structure and mechanical properties of high-entropy alloys based on CoCrFeNi system, Journal of Alloys and Compounds, 591(5): 11-21. https://doi.org/10.1016/j.jallcom.2013.12.210.
13. **Raghavan, V.** 2007. Al-Mg-Si (Aluminium-Magnesium-Silicon), Journal of Phase Equilibria & Diffusion, 28(2):189-191. https://link.springer.com/article/10.1007%2Fs11669-007-9027-8. https://doi.org/10.1007/s11669-007-9027-8.
14. **Oter, Z. C.; Gencer, Y.; Tarakci, M.** 2015. The characterization of the coating formed by Microarc oxidation on binary Al–Mn alloys, Journal of Alloys and Compounds, 650: 185-192. https://doi.org/10.1016/j.jallcom.2015.06.080.
15. **Liu, D.; Zhang, H.; Li, Y.** et al. 2017. Effects of composition and growth rate on the microstructure transformation of β-rods/lamellae/α -rods in directionally solidified Mg-Li alloy, Materials & Design, 119:199-207. http://www.jinyueya.com/magazine/41290403.htm. https://doi.org/10.1016/j.matdes.2017.01.074.
16. **Janse, J.; Zhuang, L.; Mooi, J.** et al. 2002. Evaluation of the effect of Cu on the paint bake response of preaged AA6xxx, Materials Science Forum, 396-402 (2) :607-612. https://zh.scientific.net/MSF.396-402.607.
17. **Miao, W.; Laughlin, D.** 2000. Effects of Cu content and preaging on precipitation characteristics in aluminium alloy 6022, Metallurgical and Materials Transactions A, 31 (2): 361-371. https://www.mendeley.com/research-papers/effect-cu-content-preaging-precipitation-characteristics-aluminium-alloy-6022/. https://doi.org/10.1007/s11661-000-0272-2.
18. **Wu, Y., Xiong, J., Lai, R.** et al. 2009. The microstructure evolution of an Al–Mg–Si–Mn–Cu–Ce alloy during homogenization, Journal of Alloys and Compounds, 475 (1): 332-338. http://Flink.springer.com%13800268407650515623.
19. **Allam, A., Boulet, P., Nunes, C.** et al**.** 2013. Phase transformations in higher manganese silicides, Journal of Alloys and Compounds, 551 (5): 30-36. https://www.researchgate.net/publication/257361370. https://doi.org/10.1016/j.jallcom.2012.10.016.
20. **Berche, A., Ruiz-Theron, E., Tedenac, J-C.** et al. 2014. Thermodynamic description of the Mn–Si system: an experimental and theoretical work, Journal of Alloys and Compounds, 615 (10): 693-702. https://doi.org/10.1016/j.jallcom.2014.06.202.
21. **Aremo, B., Adeoye, M.** 2010, A low-cost vacuum casting equipment for aluminium alloys, Russian Journal of Non-Ferrous Metals, 51 (2): 124-130. https://www.researchgate.net/publication/225412946_A_low_cost_vacuum_casting_equipment_for_aluminium_alloys. https://doi.org/10.3103/S1067821210020094.
22. **Alexander, D.; Greer, A.** 2002. Solid-state intermetallic phase tranformations in 3XXX aluminium alloys, Acta Materialia, 50 (10): 2571-2583. https://doi.org/10.1016/S1359-6454(02)00085-X.
23. **Niu-Can, L.; Jun-Qing, L., Ming-Sheng, Y.** 2011. Influence of RE and Mn Additions on Fe-containing Phase in Al-Si Alloys, Foundry Technology, 32 (11): 1532-1534. http://www.ixueshu.com/document/0c07b365b0a53057318947a18e7f9386.html.

24. **Mondolfo, L F.** 2013. Aluminum alloys: structure and properties, Butterworths, 31 (11) :651-657. https://www.researchgate.net/publication/236121197_Aluminum_alloys_structure_properties.
25. **Chen, A.; Zhang, L.; Wu, G.** et al. 2017. Influences of Mn content on the microstructures and mechanical properties of cast Al-3Li-2Cu-0.2 Zr alloy, Journal of Alloys and Compounds, 715: 421-431. https://doi.org/10.1016/j.jallcom.2017.05.030.
26. **Liu, Gang., Liu, Lin., Zhao, Xinbao.** 2010. A High Temperature Gradient Directionally Solidified Microstructure and Dendritic Segregation of a Ni-base Single Crystal Superalloy, Acta Metallurgica Sinica, 46 (1): 77-83. http://www.ams.org.cn/CN/Y2010/V46/I1/77.
27. **Wang, K F., Guo J. J., LY.** 2007. Numerical Simulation of Effect of Temperature Gradient on Directional Solidification Microstructure Evolution of Ti-45Al Alloy, Materials Engineering ,7 (2): 6-11. http://www.oalib.com%5858652795152860304.
28. **Si, N. C.; Xu, N. J.; Si, S. H.** 2011. Effect of temperature gradient on primary dendritic spacing of Al-4.5% Cu alloy with directional solidification, Materials Engineering, 4 (16): 75-79. http://www.ixueshu.com/ 8c63d6830552cbf0.html.
29. **Xiao, Zhi-Bin; Zheng, Li-Jing; Yan, Li-Li.** 2010. Effects of Temperature Gradient on Orientation of Directionally Solidified TiAl Based Alloy, Acta Metallurgica Sinica, 46 (10): 1223-1229. http://jme.biam.ac.cn/CN/article/downloadArticleFile.do?attachType=PDF&id=7017. https://doi.org/10.3724/SP.J.1037.2010.01223.
30. **Zhang, Qing-mao; Liu, Wen-jin; Yang. Sen.** 2001. Passice spacing of Cu-Mn alloy with high temperature gradient and rapid orientation solidification, Journal of Nonferrous Metals, 11 (2): 243-247. http://www.ixueshu.com/document/139a55e0a01f45e7318947a18e7f9386.html.
31. **Wu, Qiang; SI Nai-tao; Guo, Yi.** 2007. Effects of Dendritic Microstructures and Drawing Rate on Directionally Solidified Al-4.5% Cu Alloys, Journal of Nonferrous Metals, 17 (7): 1101-1106. http://www.ixueshu.com/document/ce5d827893cb8361318947a18e7f9386.html.
32. **Wu, Qiang; Si, Nai chao; Guo, Yi.** 2007. Effects of Dendritic Microstructures and Drawing Rate on Directionally Solidified Al-5% Cu Alloys, Journal of Nonferrous Metals, 17 (7): 1101-1106. http://www.ixueshu.com/document/ce5d827893cb8361318947a18e7f9386.html.
33. **Wang, Kuang-Fei; Guo, Jing-Jie; Lei, Chang-Yun.** 2007. Numerical Simulation of Effect of Drawing Speed on Directional Solidification Structure Evolution of Ti-45Al Alloy, Foundry, 56 (11): 1186-1199. http://www.cqvip.com/read/read.aspx?id=26014464.
34. **Luo Wen zhong; Shen Jun; Li Qinglin.** 2006. Effects of Drawing Rate on Directional Solidification Structure of Ti-43Al-3Si Alloy Seed Crystals, Acta Metallurgica Sinica, 42 (12): 1238-1242. http://www.cqvip.com/read/read.aspx?id=23490222.

Tao He, Li Min, Yuan ming Huo, Hong Jun Liu, Xiao Jie Yi

EFFECT OF TEMPERATURES AND PULLING RATES ON MICROSTRUCTURE AND MECHANICAL PROPERTIES OF 6061 ALUMINUM ALLOY IN DIRECTIONAL SOLIDIFICATION

S u m m a r y

During directional solidification, temperatures and pulling rates have significant influences on microstructure of casting rods. And, mechanical properties of 6061 aluminum alloy rods depend on microstructure formed in the directional solidification. In order to study the effect of temperatures and pulling rates on microstructure and mechanical properties, the directional solidification experiment of 6061 aluminum alloy were performed using Bridgman-type vacuum furnace with liquid metal cooling(LMC) method at different temperatures (700°C, 750°C and 800°C) and pulling rates (20 μm/s, 50 μm/s, 100 μm/s and 150 μm/s). Microstructural investigation of 6061 aluminum alloy rods was performed using Hitachi SU8070 SEM. And, tensile tests and microhardness tests were conducted on JVJ–50s test machine and MHVD-1000IS hardness tester separately. Experimental results indicate that the dendritic structure of the specimen gradually is refined uniformly, and the intergranular spacing becomes smaller with the increase of temperatures. Some defects lead to the decline of mechanical properties of alloy with the increase of temperatures. The tensile strength at the temperature of 750 °C is the highest, reaching 182.51 MPa. However, the microhardness at the temperature of 800°C is the highest, reaching 56.77 HV. When the pulling rate is 50 μm/s, the tensile strength shows better than that at the pulling rate of 100 μm/s and 150 μm/s, reaching 183.31 MPa. However, the highest microhardness takes places at the pulling rate of 150 μm/s, reaching 67.66 HV.

Keywords: directional solidification, liquid metal cooling, 6061 aluminum alloy, microstructure, mechanical properties.

Received September 28, 2017
Accepted February 15, 2018